

Sliding and dry friction: Prandtl-Tomlinson athermal model revisited

María Luján Iglesias · Sebastián Gonçalves

July 24, 2020

Abstract The microscopic origin of friction has been the goal of several theoretical studies in the last decades. Depending on the investigated systems or models, on the simulation techniques or conditions, different and somewhat contradictory results have been found, even when using the same model. In this contribution we address this apparent paradox in a well know case, the Prandtl-Tomlinson model at zero temperature, studying the force-velocity relation for a wide range of velocities not previously presented. Including much more data density for the non trivial regions, we are able to shed light on this problem and at the same time, provide new insight in the use of the paradigmatic Tomlinson model for the secular problem of friction laws.

Keywords microscopic friction · nanotribology · Prandtl-Tomlinson model

1 Introduction

What are the precise microscopic mechanisms that causes the appearance of *friction forces* at the macroscopic level is one of the oldest problems in physics, whose fundamental origin has been studied for centuries and still remains controversial [1, 2, 3]. Our hominid ancestors in Algeria, China, and Java (more than 400,000 years ago) made use of friction when they chipped stone tools [4], for example. Around 200,000 years ago, Neanderthals generated fire by the rubbing of wood on wood or by the striking of flint stones. Significant developments occurred some 5,000 years ago, as an Egyptian tomb drawing suggests that wetting the sand with water to lower the friction between a sled and the sand [5] was used for moving large rocks.

María Luján Iglesias
Instituto de Física, Universidade Federal do Rio Grande do Sul
Caixa Postal 15051
91501-970
Porto Alegre RS, Brazil. E-mail: lujaniglesias@gmail.com

Sebastião Gonçalves
E-mail: sgonc@if.ufrgs.br

The scientific formalization of such empirical knowledge started with Da Vinci, followed by Amontons and Coulomb. They established that the friction experienced by a body in contact with an even surface is proportional to the load. Second, the amount of friction force does not depend on the apparent area of contact of the sliding surfaces. And third, the friction force is independent of velocity, once motion starts [6, 7]. These three laws, commonly verified in a macroscopic scale, are the result of the collective behavior of many single asperity contacts, as was shown by Bowden and Tabor(1954) [8].

With the introduction of the atomic force microscope (AFM) [9] and friction force microscope (FFM) [10], Bowden and Tabor’s theory could be experimentally verified, proving that friction laws for a single asperity are different from macroscopic friction laws. One of the main results, confirmed by several experiments [10, 11], is that the friction force on the nanometer scale exhibits a saw-tooth behavior, commonly known as “stick-slip” motion. This observation can be theoretically reproduced within classical mechanics using the Prandtl-Tomlinson model [12].

Over many years, this model has been referred as the “Tomlinson model” even though the paper by Tomlinson did not contain it. In fact, it was Ludwig Prandtl who suggested in 1928 a simple model for describing plastic deformation in crystals [13]. His contributions were more associated with fluid mechanics [14], mechanics of plastic deformations, friction, and fracture mechanics [15]. In order to correct this historical error, in 2003 Müser, Urbakh, and Robbins, published a fundamental paper [16] in which the mentioned model was termed “Prandtl-Tomlinson Model” [17]. Indeed, the Prandtl-Tomlinson (PT) model has received some renewed attention, as can be seen for example in modeling the aging effect on friction at the atomistic scale [18].

On the other side, Makkonen [3], using a thermodynamic approach, relates friction to the surface energy involved at the edges of nanoscale contacts between materials, as the result of new surface formation. This is a different approach as compared with the Prandtl-Tomlinson model presented here, which assumes that friction arises within the nanocontacts.

In the last years, theoretical predictions for the atomic friction, based on the Prandtl-Tomlinson and Frenkel-Kontorova [19, 20, 21] models, were proposed. The advantage of such models resides in being simple and yet retaining enough complexity to show interesting features. Such models were able to explain some features of atomic-scale friction, relating the energy dissipation with the stick-slip motion, atomic vibration, and resonance [22, 23, 24, 25, 26, 27].

In the original experiments of Mate *et al.* [10] the authors state that the frictional force of a tungsten tip on graphite shows little dependence on velocity for scanning velocities v_c up to 400 nm/s. A similar behavior has been reported in the work of Zwornier *et al.* [28] for velocities up to several $\mu\text{m/s}$, where friction on different carbon structures has been studied. They claim that a 1D Prandtl-Tomlinson model at $T = 0$ can reproduce the velocity independent friction force for scanning velocities up to 10 $\mu\text{m/s}$, while giving rise to linear increase of friction for higher velocities. Other works claim a logarithmically increase in the friction force with velocity, attributed to thermal activation [29, 30, 31, 32, 33, 34, 35]. Fusco and Fasolino [25] have shown that an appreciable velocity dependence of the friction force, for small scanning velocities (from 1 nm/s to 1 $\mu\text{m/s}$), is inherent to the Prandtl-Tomlinson model, having the form of a power-law $F_{fric} - F_0 \propto v_c^{2/3}$. Con-

sidering the variety of seemingly controversial results, we conducted the present study, producing a wide range of numerical data for the friction force as a function of the scanning velocity. With a higher density of points it is possible to identify four clearly behavioral regions, which may go unnoticed depending on how the data is presented.

In this way, we show the results in different scales of representations to demonstrate how the conclusions appear to be conflicting. At the same time, an overlooked region of data shows an interesting behavior not previously reported.

2 Methodology

We use the 1D Prandtl-Tomlinson model at $T = 0$ to simulate a tip of mass m attached by a spring of constant k to a support (cantilever) moving at constant velocity v_c along the X direction, over a surface represented by a periodic potential $V(x)$, where x represents the position of the tip. A graphical representation of the model is shown in Fig. 1.

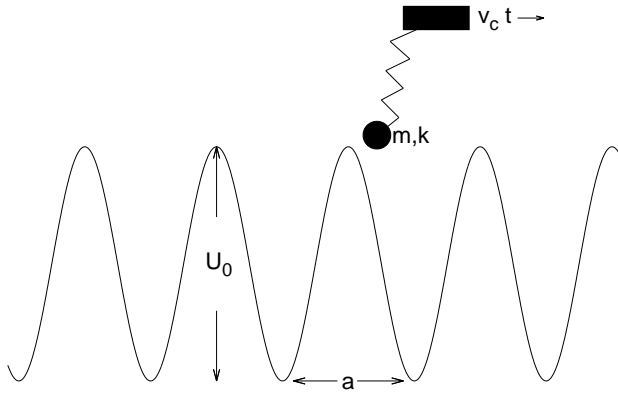


Fig. 1 Sketch of the 1D Prandtl-Tomlinson model for atomistic friction. The cantilever tip of mass m and constant K is moving at constant velocity v_c . The surface is represented as a potential with corrugation U_0 and period a

The interaction potential has the form

$$V(x) = U_0 \cos\left(\frac{2\pi x}{a}\right), \quad (1)$$

where a is the lattice spacing. The elastic interaction between the tip and the support is

$$V_{el}(x) = \frac{1}{2}k(x - x_c)^2, \quad (2)$$

where $x_c = v_c t$ is the equilibrium position of the spring. Thus, the equation of motion for this system, including the *ad-hoc* dissipation term, is

$$m \frac{d^2 x}{dt^2} = -k(v_c t - x) + U_0 \frac{2\pi}{a} \sin\left(\frac{2\pi}{a} x\right) - m\gamma \frac{dx}{dt}, \quad (3)$$

The term proportional to the tip velocity $\frac{dx}{dt}$ is added to introduce energy dissipation in the model. Being γ this proportionality constant. Equation 3 represent the same model used in some previous contribution to which we want to make contact [25,28].

The lateral force F is calculated as $F = k(x_c - x)$, whereas the frictional force F_{fric} is identified as the lateral force averaged over time $\langle F \rangle$ [36]. We solve the nonlinear equation 3, using the velocity Verlet algorithm [37] for a wide range of scanning velocity v_c .

3 Results

In this section we present the results obtained by solving numerically the equation of motion (Eq. 3) for the Prandtl-Tomlinson model. The values of the constants for the model are: $k = 10 \text{ N/m}$, $m = 10^{-10} \text{ kg}$ (which gives a natural frequency for the tip, $\sqrt{k/m} \simeq 316 \text{ kHz}$), and $a = 0.3 \text{ nm}$, typical values of AFM experiments [30, 38, 28, 25]. In general, the amplitude used for the corrugation U_0 goes from 0.2 to 2 eV [32], and in the present case we use $U_0 = 1 \text{ eV}$. We chose $\gamma = 2\omega = 2\sqrt{k/m}$ in order to have critical resonance of the system, and the time step used for the numerical integration was $\Delta t \simeq 1 \text{ ns}$ ¹. These particular set of parameters were chosen in order to compare our results with those obtained by Zworner *et al.* [28] and Fusco and Fasolino [25].

With the help of the software Engauge Digitizer [39] we recover the data points from the graphics of the mentioned references; in this way we can reproduce the plots of their simulations in the most similar way to the original articles. Figure 2 (left and right) reproduces the results of Fusco and Fasolino [25] for linear and log-log scale, and Fig. 3 the corresponding ones of Zworner *et al.* [28].

Moreover, with the digitized data at hand, we can put the two sets in the same graph along with the results from our own simulations (as shown in Fig. 4), so we can compare the three set of data in the different regions.

Our numerical results are extended down to 0.1 nm/s, in order to show that, in principle, all data seems to be consistent. It can be appreciated from the plot in linear scale (Fig. 4 left), that this consistency is hard to appreciate, particularly under $1 \mu\text{m/s}$ where many order of magnitude are condensed. For this reason, the same data has to be presented in a more convenient scale, which is the case of a semi-log scale (Fig. 4 right).

Zworner *et al.* [28] use a wide range of velocities (from $10^{-2} \mu\text{m/s}$ to $10^3 \mu\text{m/s}$) so it is interesting to analyze in detail the results on different regions.

In their work, the authors concluded that the model exhibits two limiting behaviors for the resulting frictional force (Fig. 3): a velocity independent regime at

¹ The period of oscillation of the cantilever is $20 \mu\text{s}$ and the maximum simulated speed is 1 mm/s , so that time step is more that 1000 times smaller that the period and at the maximum speed it moves only 1/300 of the potential length

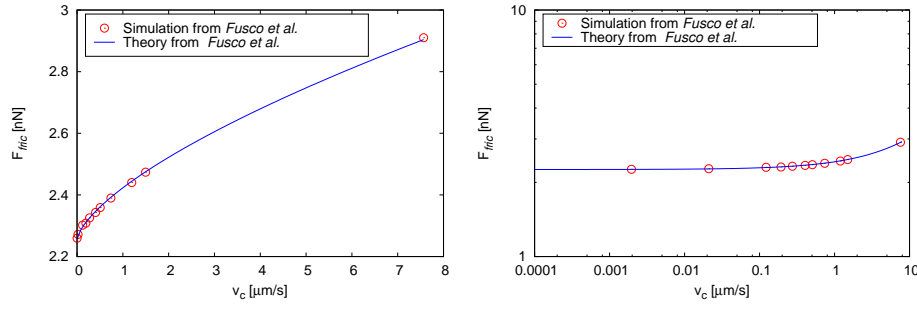


Fig. 2 Data extracted from Fusco and Fasolino [25] showing the friction force (F_{fric}) as a function of the sliding velocity (v_c), plotted on a linear (top) and on a log-log scale (bottom), in the same way it was presented in the original article.

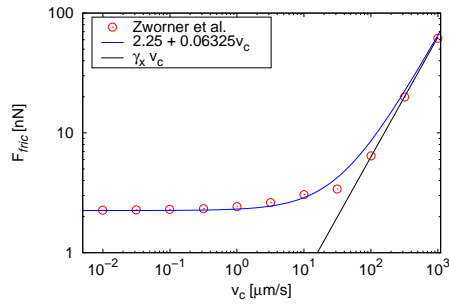


Fig. 3 Data extracted from Zworner *et al.* [28] showing the frictional force (F_{fric}) as a function of the sliding velocity (v_c), along with the analytic expressions proposed by them for the two limiting regimes.

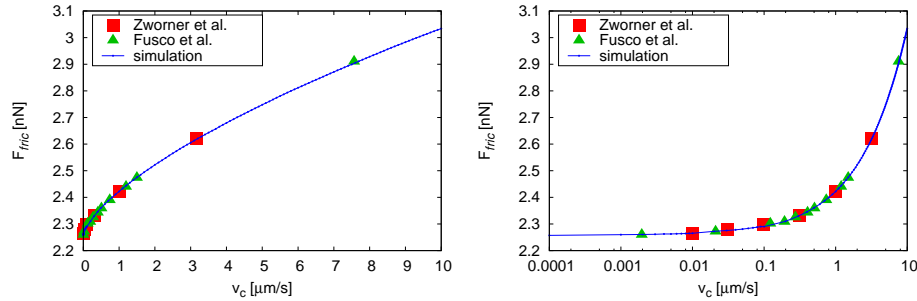


Fig. 4 F_{fric} as a function of v_c in semi-log scale; comparison between previous and present numerical results with the athermal Prandtl-Tomlinson model: Zworner *et al.* [28], Fusco and Fasolino [25], and present contribution.

low velocities, below $1 \mu\text{m/s}$ and a viscous linear regime for velocities $\geq 100 \mu\text{m/s}$. We can see in Fig. 5 that these two limiting cases—and particularly the combination of both— can give an approximated description of the Prandtl-Tomlinson

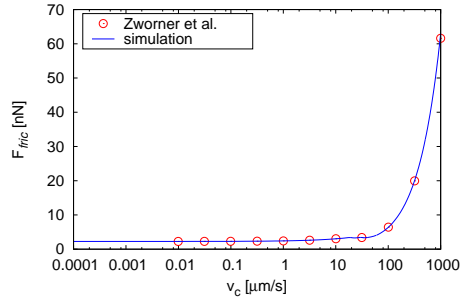


Fig. 5 F_{fric} as a function of v_c in linear and semi-log scale; comparison between Zworner *et al.* [28] simulations and present numerical results with the athermal Prandtl-Tomlinson model.

model results in the wide region of velocities displayed. However, one has to be aware that the log-log scale used to present the data might hide possible departures from such behavior, providing an oversimplification of the otherwise rich features of the Prandtl-Tomlinson model that we will show in section 3.2

According with Zworner *et al.* interpretation there is no change in the frictional force when the velocity goes from 10 nm/s to 1 μ m/s. After this, F_{fric} is proportional to γv_c in a viscous damping regime. Our results were done in a wide interval of velocities, covering both previous papers ranges and more, plus a small velocity increment. Displaying the data in a linear scale (Fig. 6, left), and with a higher density of points, we can see that the dependence is far from being constant. Moreover, on Fig. 6 right, we show how the choice of the scale can influence on the data interpretation, hiding relevant aspects of the behavior of the system.

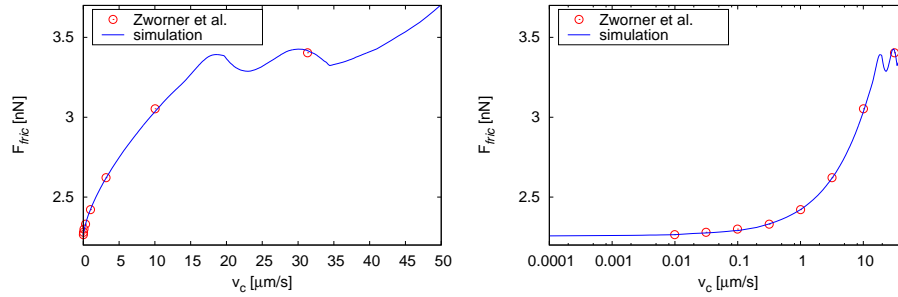


Fig. 6 Comparison between data from Zworner *et al.* [28] and from present contribution in linear and semi-log scale.

3.1 Small Velocities representation

For small velocities (up to $1 \mu\text{m/s}$) we also make contact with the results of Fusco and Fasolino [25] by comparing the results of our own simulations with the digitized data from them in Fig. 7.

In their article, the authors develop an approximation to the dependence of the frictional force with the velocity, showing that F_{fric} follows a power law of the form:

$$F_{fric} = F_0 + cv_c^{2/3} \quad (4)$$

where c is a constant that depends on the parameter of the model and on the space dimension. This approximation is very accurate for this range of velocities. Highlighting again that the friction is not independent of the velocity. This proves that depending on the scale chosen to represent the data, important information can be overlooked. The same Figure also shows that this power-law dependency continues to be valid for higher velocities of up to $20 \mu\text{m/s}$.

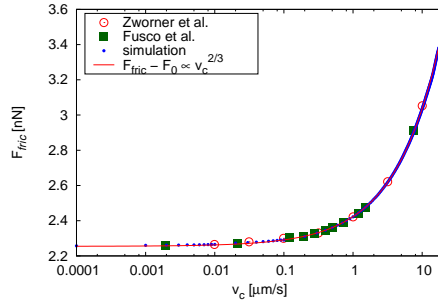


Fig. 7 Increase of the frictional force with velocity between $10^{-3} \mu\text{m/s}$ to $20 \mu\text{m/s}$. The line is a power-law fit to the data of the form $F_{fric} - F_0 \propto v_c^{2/3}$. [25]

3.2 Transitional and Large Velocities representation

An important fact that stands out is the distinctive behavior in the region between $10 \mu\text{m/s}$ and $35 \mu\text{m/s}$ (Fig. 10), where F_{fric} oscillates with v_c around a fixed value of force. Indeed, for the velocities v_c in this region, the tip sees a force from the surface that varies with the a frequency close to its own natural frequency [24, 40], *i.e.*:

$$v_c^{res} = \frac{a}{2\pi} \sqrt{\frac{k}{m}} \simeq 15 \mu\text{m/s} \quad (5)$$

In order to better understand what could be the origin of the reported behavior we present below the tip position and velocity as a function of the cantilever position (Fig. 8). We present that data for different values of the sliding cantilever velocity. For velocities well below the region where friction oscillates, we have the typical stick-slip behavior where energy dissipates mainly after the slip movement.

For large velocities the viscous regime is recovered. However in the region of interest we observe that the tip slips over a distance of two cell parameters, from one potential barrier to the second other one. This happens only for a damping coefficient near critical. Then, instead of being a resonance phenomenon, it is a critical damping effect where the dissipation remains at its minimum compatible with the sliding speed (Fig. 9). The presence of double jumps for that range of velocities, makes us to wonder if multiple (more than two) slide jumps would be possible. That can happen, depending on the key parameters of the model, *i.e.*, U_0 , k , and a [41], and it deserves a future and thorough analysis.

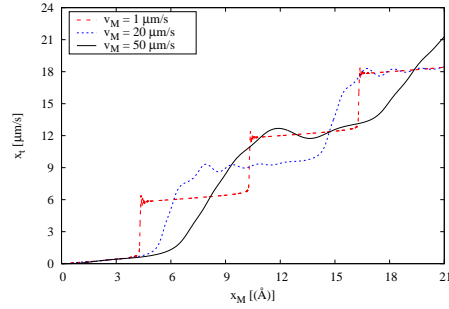


Fig. 8 Tip position as a function of cantilever position for different sliding velocities, before, at, and after the region where friction oscillates.

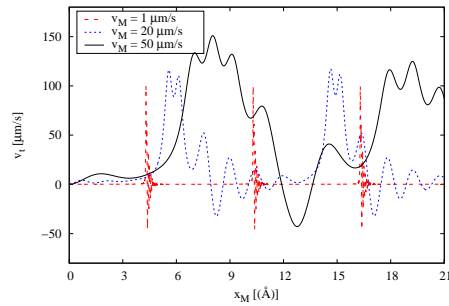


Fig. 9 Tip velocity as a function of cantilever position for different sliding velocities, before, at, and after the region where friction oscillates.

Such behavior comes to light in reason of the remarkable increase in the density of simulated points and it has not been reported before. In this segment the value of F_{fric} oscillates around an average value of 3.35 nN. This behavior goes totally unnoticed in a logarithmic representation of the data. Some recent experiments [43, 44] have been carried out evaluating the friction dependence on speed near this region, but without covering the entire range and without sufficient detail and precision.

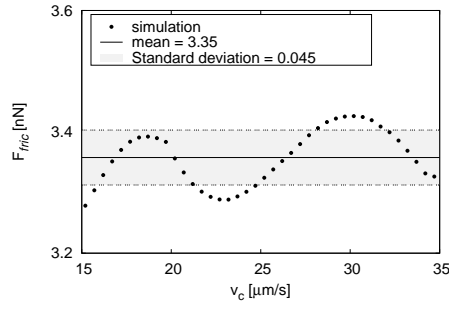


Fig. 10 Detail of the behavior of the friction force with velocity between 15 to 35 $\mu\text{m/s}$. We can say that friction is stationary in this range of velocities.

After the transition region, we observe that friction grows again. We fit the data with a quadratic power-law:

$$F_{fric} - F \propto v_c^2 \quad (6)$$

where F is the value of the friction at the lower velocity of the adjustment (Fig. 11). The quadratic growth fits very well with the simulation data up to 0.1 mm/s behaving like a drag force until finally, for large sliding velocities, the mechanism of energy dissipation through the “stick-slip” effect breaks down, and F_{fric} is proportional to γv_c , where critical damping is assumed, giving $\gamma = 2\sqrt{km}$.

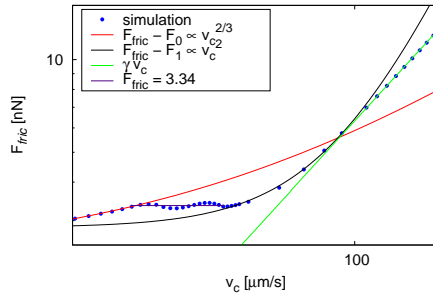


Fig. 11 The friction force as a function of velocity in the transition region between the low velocities $v_c^{2/3}$ regime to the high velocities, viscous linear regime. For that intermediate regime of velocities the force goes through two other transitional regimes of almost constant force to quadratic velocity regime before entering the linear regime. Increase of the frictional force with velocity between 35 to 100 $\mu\text{m/s}$. The line is a power-law fit to the data of the form $F_{fric} - F \propto v_c^2$. For high velocities the frictional force is proportional to the velocity in the regime of viscous damping

4 Conclusion

We have presented a thorough numerical study on the velocity dependence of friction that emerge from the classical Prandtl-Tomlinson model in the athermal case.

Despite the fact that similar works have already been carried out, our contribution was made with a higher density of points, bringing to light behaviors not previously reported. By comparing our results with previous ones with the same model, we were able to conciliate apparent conflicting results while providing new insight and interpretation of them. Besides, we present results in regions not previously explored. We confirm Fusco and Fasolino results for small velocities but extended up to $15\ \mu\text{m/s}$, where friction force has a dependence of $v_c^{2/3}$. A transition region located between $15\text{--}35\ \mu\text{m/s}$ where there is a constant frictional force on average and then an increase proportional to v_c^2 up to $100\ \mu\text{m/s}$. After this, the force is proportional to γv_c in a viscous damping regime. Our numerical study shows that depending on how the results are presented, mainly when changing from linear scale to logarithmic, part of this rich and interesting behavior can go unnoticed.

Acknowledgements This work was supported by the Centro Latinoamericano de Física (CLAF), the Conselho Nacional de Desenvolvimento Científico e Tecnológico (CNPq, Brazil) and in part by the Coordenação de Aperfeiçoamento de Pessoal de Nível Superior - Brasil (CAPES) - Finance Code 001.

References

1. B.N.J. Persson, Sliding Friction Physical Principles and Applications, Springer-Verlag Berlin Heidelberg, 2000.
2. J. Krim, Surface science and the atomic-scale origins of friction: what once was old is new again, Surface Science, 500(1–3):741 – 758, 2002.
3. L. Makkonen, A thermodynamic model of sliding friction, AIP Advances, 2(1):012179, 2012.
4. B. N. J. Persson, Sliding Friction: Physical Principles and Applications, Springer Berlin Heidelberg, 2013.
5. A. Fall, B. Weber, M. Pakpour, N. Lenoir, N. Shahidzadeh, J. Fiscina, C. Wagner and D. Bonn, Sliding Friction on Wet and Dry Sand, Phys. Rev. Lett., 112(17):2014.
6. T. Baumberger, Dry Friction Dynamics at Low Velocities, Springer Science Business Media, 1996.
7. M. H. Müser, L. Wenning, and M. O. Robbins, Simple Microscopic Theory of Amontons’s Laws for Static Friction, Phys. Rev. Lett., 86(7):1295–1298, 2001.
8. F. P. Bowden, The Friction and Lubrication of Solids, Am. J. Phys., 19(7):428, 1951.
9. G. Binnig, C. F. Queswade and Ch. Gerber, Atomic Force Microscope, Phys. Rev. Lett., 56(9):930–933, 1986.
10. C. M. Mate, G. M. McClelland, R. Erlandsson, and S. Chiang, Shirley, Atomic-scale friction of a tungsten tip on a graphite surface, Phys. Rev. Lett., 59(17):1942–1945, 1987.
11. S. Fujisawa, E. Kishi, Y. Sugawara, and S. Morita, Atomic-scale friction observed with a two-dimensional frictional-force microscope, Phys. Rev. B, 51(12), 7849–7857, 1995.
12. G.A. Tomlinson, CVI. A molecular theory of friction, The London Edinburgh, and Dublin Philosophical Magazine and Journal of Science, 7(46):905–939, jun 1929.
13. L. Prandtl, Ein Gedankenmodell zur kinetischen Theorie der festen Körper. ZAMM 8, 85–106, 1928.
14. L. Prandtl, Über Flüssigkeitsbewegung bei sehr kleiner Reibung, Verhandlungen III, p. 484, Intern. Math. Kongress, Heidelberg, 1904.
15. L. Prandtl, Über die Härte plastischer Körper, Nachrichten Göttinger Akad. Wiss., 1920.
16. M. H. Müser, M. Urbakh, M.O. Robbins, Statistical mechanics of static and low-velocity kinetic friction. In: Prigogine, I., Rice, S.A. (eds.) Advances in Chemical Physics, vol. 126, pp. 187–272, 2003.
17. V. Popov, and J.A.T. Gray, Prandtl-Tomlinson Model: A Simple Model Which Made History, ISBN 978-3-642-39904-6 153–168, jan 2014
18. J.J. Mazo, D. Dietzel, A. Schirmeisen, J.G. Vilhena, and E. Gnecco, Time Strengthening of Crystal Nanocontacts Phys. Rev. Lett., 118 (24), Jun 2017.

19. T. Kontorova and J. Frenkel, On the theory of plastic deformation and twinning II, *Zh. Eksp. Teor. Fiz.*, 8:1340–1348, 1938.
20. J. Frenkel and T. Kontorova, On the theory of plastic deformation and twinning, *Izv. Akad. Nauk, Ser. Fiz.*, 1:137–149, 1939.
21. O.M. Braun and Y.S. Kivshar, *The Frenkel-Kontorova Model: Concepts, Methods, and Applications*, Physics and Astronomy Online Library. Springer, 2004.
22. A. Buldum and S. Ciraci, Atomic-scale study of dry sliding friction, *Phys. Rev. B*, 55: 2606–2611, Jan 1997.
23. S. Gonçalves, V. M. Kenkre, and A. R. Bishop, Nonlinear friction of a damped dimer sliding on a periodic substrate, *Phys. Rev. B*, 70(19), nov 2004.
24. S. Gonçalves, C. Fusco, A. R. Bishop, and V. M. Kenkre, Bistability and hysteresis in the sliding friction of a dimer, *Phys. Rev. B*, 72:195418, Nov 2005.
25. C. Fusco and A. Fasolino, Velocity dependence of atomic-scale friction: A comparative study of the one- and two-dimensional Tomlinson model, *Phys. Rev. B*, 71(4), Jan, 2005.
26. M. Tiwari, S. Gonçalves, and V. M. Kenkre, Generalization of a nonlinear friction relation for a dimer sliding on a periodic substrate, *The European Physical Journal B*, 62(4): 459–464, apr 2008.
27. I. G. Neide, V. M. Kenkre, and S. Gonçalves, Effects of rotation on the nonlinear friction of a damped dimer sliding on a periodic substrate, *Physical Review E*, 82(4), oct 2010.
28. O. Zwornier, H. Holscher, U.D. Schwarz, and R. Wiesendanger, The velocity dependence of frictional forces in point-contact friction, *Applied Physics A: Materials Science & Processing*, 66(7), S263–S267, 1998.
29. T. Bouhacina, J.P. Aimé, S. Gauthier, D. Michel, and V. Heroguez, Tribological behavior of a polymer grafted on silanized silica probed with a nanotip, *Phys. Rev. B*, 56(12), 7694–7703, 1997.
30. R. Bennewitz, T. Gyalog, M. Guggisberg, M. Bammerlin, E. Meyer, and H. J. Güntherodt, Atomic-scale stick-slip processes on Cu(111), *Phys. Rev. B*, 60(16), R11301–R11304, 1999.
31. E. Gnecco and R. Bennewitz and T. Gyalog and Ch. Loppacher and M. Bammerlin and E. Meyer and H.-J. Güntherodt, Velocity Dependence of Atomic Friction, *Phys. Rev. Lett.*, 84(6), 1172–1175, 2000.
32. E. Riedo, E. Gnecco, R. Bennewitz, E. Meyer, and H. Brune, Interaction Potential and Hopping Dynamics Governing Sliding Friction, *Phys. Rev. Lett.*, 91(8), Aug, 2003.
33. L., Qunyang, D. Yalin, D. Perez, A. Martini, and R. W. Carpick, Speed Dependence of Atomic Stick-Slip Friction in Optimally Matched Experiments and Molecular Dynamics Simulations, *Phys. Rev. Lett.*, 106(12), Mar, 2011.
34. K. B. Jinesh, S. Y. Krylov, H. Valk, M. Dienwiebel, and J. W. M. Frenken, Thermolubricity in atomic-scale friction, *Phys. Rev. B*, 78(15), Oct, 2008.
35. Y. Sang, M. Dubé, and M. Grant, Thermal Effects on Atomic Friction, *Phys. Rev. Lett.*, 87(17), Oct, 2001.
36. D. Tománek, W. Zhong and H. Thomas, Calculation of an Atomically Modulated Friction Force in Atomic-Force Microscopy, *Europhysics Letters (EPL)*, 15(8), 887–892, 1991.
37. L. Verlet, Computer Experiments on Classical Fluids. II. Equilibrium Correlation Functions, *Phys. Rev.*, 165(1), 201–214, 1968.
38. H. Hölscher and U.D. Schwarz and R. Wiesendanger, Modelling of the scan process in lateral force microscopy, *Surface Science*, 375(2-3), 395–402, 1997.
39. Engauge Digitizer, <https://markummittchell.github.io/engauge-digitizer/>, note = Accessed: 2018-09-24
40. C. Apostoli, G. Giusti, J. Ciccianni, G. Riva, R. Capozza, R. L. Woulaché, A. Vanossi, E. Panizon, N. Manini, *Beilstein J. Nanotechnol.*, 8:2186–2199, 2017.
41. E. Gnecco, R. Roth, and A. Baratoff, Analytical expressions for the kinetic friction in the Prandtl-Tomlinson model *Phys. Rev. B* 86, 035443, 2012.
42. E. Granato, and S. C. Ying, Non-Monotonic Velocity Dependence of Atomic Friction *Tribology Letters*, 39(3):229–233, Sep 2010.
43. J. Chen, I. Ratera, J. Y. Park, M. Salmeron, Velocity dependence of friction and hydrogen bonding effects., *Phys. Rev. Lett.* 96, 236102, 2006
44. Y. Diao, and R. Espinosa-Marzal, The role of water in fault lubrication, *Nature Communications*, Vol. 9 , 2018